EXPERIMENTS TESTING THE USE OF THE MAGNETOMETER IN DETERMINING GEOLOGIC STRUCTURE

Thesis by

Sidney Schafer

In Partial Fulfillment of the Requirements for

the Degree of Master of Science

California Institute of Technology

Pasadena, California

1936

FOREWORD

The purpose of this research was three-fold. Firstly, it was conducted in order to acquaint the author with the technique of measuring the vertical and horizontal components of the distorted earth's magnetic field and with the problems which arise during the course of a magnetic survey. Secondly, it was conducted in order to acquaint the author with the usefulness of the magnetometer as an aid to the solution of structural geology problems. Lastly, it was conducted in the hope that a contribution would be made to geologic knowledge in the field of structural geology.

Two areas were chosen for investigation. The Los Angeles Basin Area was chosen because it afforded an opportunity to study a large geologic feature, complicated by faults, about which much is well known. The second area, Antelope Valley, in the Mojave Desert, was chosen because several faults of great displacements are known, or supposed, to exist in the area and because a large portion of the area is covered by aluvium, thus affording opportunity to investigate an area about which little is known.

TABLE OF CONTENTS

PART I

MAGNETIC SURVEY OF THE LOS ANGELES BASIN

Geology

Field Studies

Theoretical considerations of the Magnetic Field across a basin-like structure.

- Introduction
- Statement of the Problem
- Solution of the Problem
  - Case I
  - Case II
- Calculations

Conclusions

Data

Footnotes

PART II

MAGNETIC SURVEY OF ANTELOPE VALLEY, CALIFORNIA

Introduction

Geography

Geology

Magnetic Survey

- Rosamand Fault
- Garlock Fault
- General Magnetic Survey of Antelope Valley

Conclusions

Data

PART I

MAGNETIC SURVEY OF THE LOS ANGELES BASIN

MAGNETIC SURVEY OF THE LOS ANGELES BASIN

GEOLOGY

The Los Angeles Basin is a broad syncline with an axial trend of northwest to southeast and is approximately 75 miles long and 35 miles wide. Figure 1 is a section across the basin from Azusa in the northeast to San Pedro Hills in the southwest. This section is based on geologic work[1], oil well data, seismic data[2], and gravity[3] measurements. It shows that the basin attains a depth of 40,000 feet at its deepest point in the vicinity of Bellflower.

Immediately overlying the basement granitic rocks is a thickness of about 15,000 feet of schists[3] and other non-crystalline metamorphic rocks of Franciscan age. On this there are about 25,000 feet of soft sandstones and shales largely of marine origin and mainly of Tertiary age. Alluvial deposits are spread over these by streams crossing the Los Angeles Plain from the mountains at the north.

The structure of the basin is somewhat complicated by high angle faults of considerable displacement. These trend in a general northwest and southeast direction.

FIELD STUDIES

Values of the vertical and horizontal components

of the magnetic field were measured with Askania magnetometers of the California Institute of Technology. The vertical component was measured at intervals of ¼ to ½ mile. The horizontal component was measured at intervals of from three to four miles.

The profile extends from the San Pedro Hills northeastward across the Signal Hill oil field and the Puente Hills to the mouth of San Gabriel Canyon in the San Gabriel Mountains. The total length is approximately 45 miles. Measurements were omitted for a distance of 2 miles across the Signal Hill Oil Field on account of the disturbance caused by the great amounts of casing and iron structures.

It was thought that it would be possible to detect the positions of the large faults that traverse the basin parallel to its major axis. These faults displace the granite at considerable depths and the vertical offsets at the shallower depths are in materials of similar permeability on both sides of the fault. As a result, no definite anomalies occur to indicate the position of the faults.

The portion of the profile between the Inglewood fault and San Pedro Hills is of decidedly anomalous character. A number of theories concerning the distribution of magnetite in the sediments or faulting might be postulated. In order to get a clearer interpretation of the profile in terms of structure, a calculation of

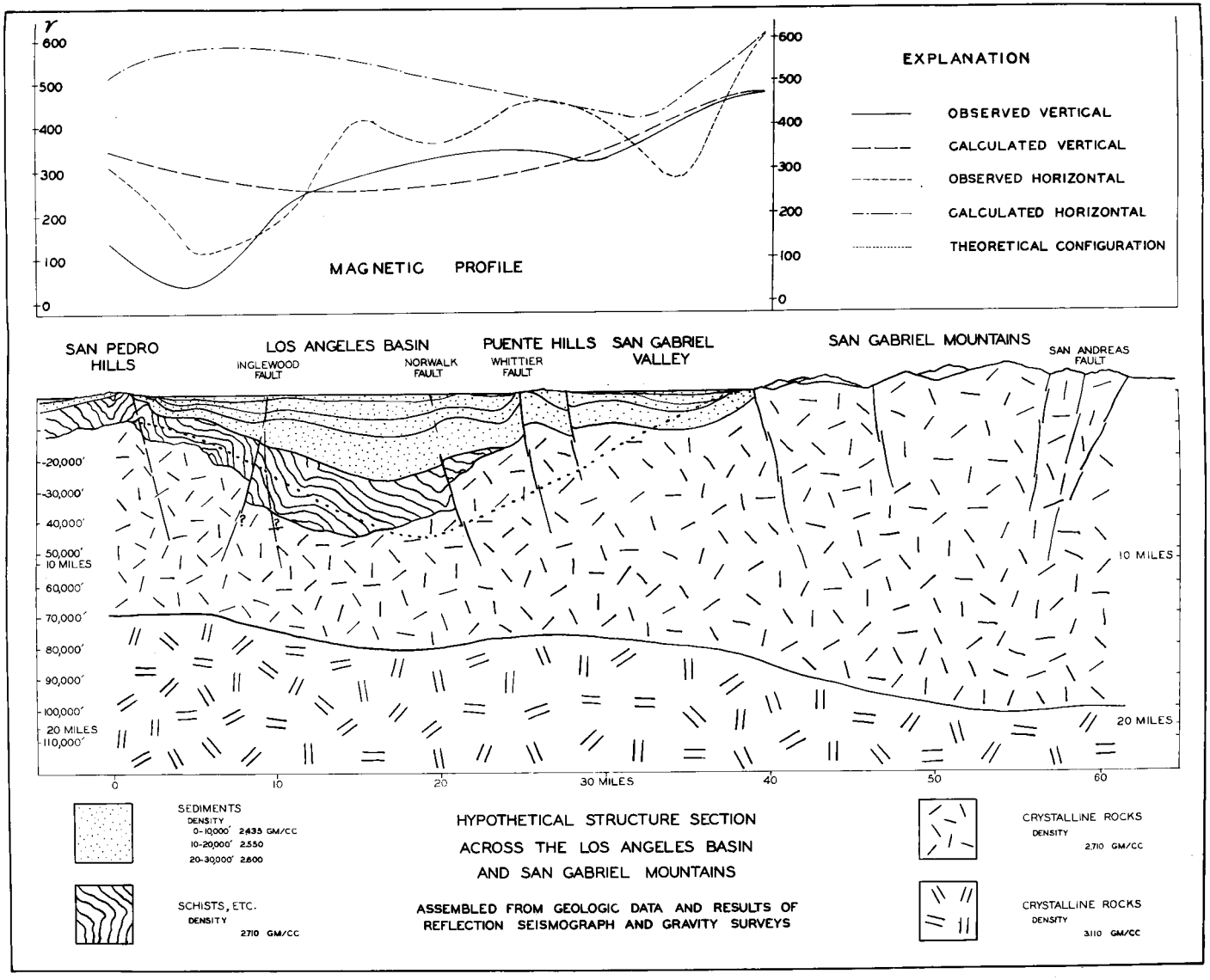

HYPOTHETICAL STRUCTURE SECTION
ACROSS THE LOS ANGELES BASIN
AND SAN GABRIEL MOUNTAINS

ASSEMBLED FROM GEOLOGIC DATA AND RESULTS OF REFLECTION SEISMOGRAPH AND GRAVITY SURVEYS

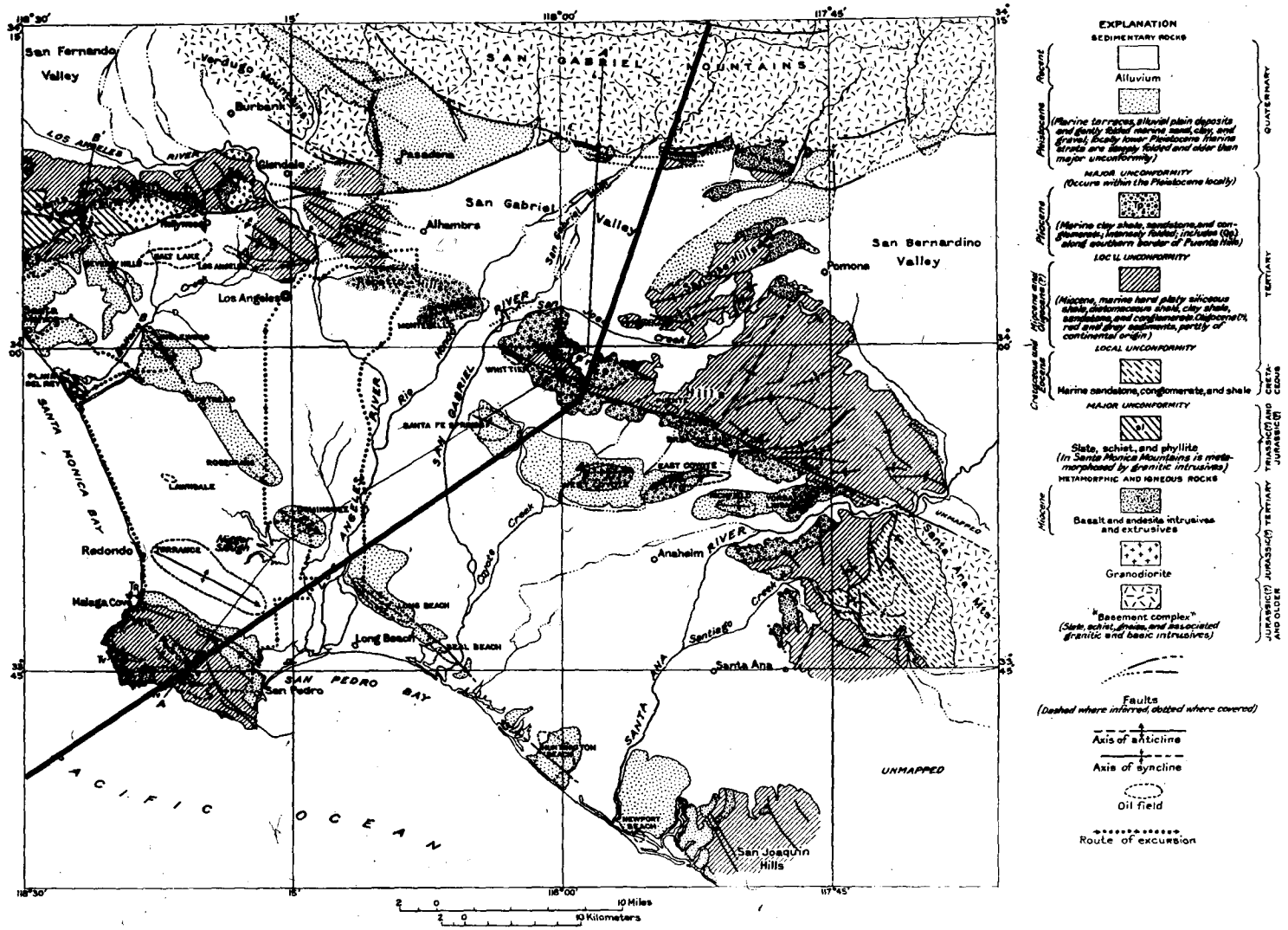

GEOLOGIC MAP OF LOS ANGELES BASIN

Compiled by H. W. Hoots and W. S. W. Kew from published and unpublished maps. Geology north of San Jose Hills from unpublished map by Rollin Eckis. For sections along lines *A–A'* and *B–B'* see Figures 1 and 2.

the field distorted by a basin-like structure was made.

THEORETICAL CONSIDERATIONS OF THE MAGNETIC FIELD ACROSS A BASIN-LIKE STRUCTURE

INTRODUCTION

Dr. W. N. Smythe outlined a method of calculating the distortion of the magnetic field caused by a basin-like structure of the dimensions of the Los Angeles Basin. L. F. Uhrig carried out the calculations as given below.

STATEMENT OF THE PROBLEM

Any attempt to rigorously find the distortion of the magnetic field by such a complicated structure as the Los Angeles Basin would be extremely difficult. In order to make this solution as simple as possible a number of approximations which are not too extreme must be made. The problem may be considered as two-dimensional and from Figure 1, one sees that it could be reduced to that of two semi-infinite blocks of different permeabilities separated by a sinousoidal boundary and placed in an inclined field. This assumes that the air, sediments, and metamorphics have the same permeability, while the granite has a different permeability. This is a safe approximation as the susceptibilities given for rocks of this region by J. L. Soske[4] are:

Clays, Gravels, Metamorphics etc. 1 to 40 x 10^{-6} C.G.S.
Granite 1000 plus x 10^{-6}

SOLUTION OF THE PROBLEM

The solution lies in finding some simple transformation that will transform a known field about a known body into the configuration wanted. The simplest bodies are the ellipse and circle which may be transformed into the Z plane by the transformation $Z = \ln Z$.

CASE I

If an ellipse is transformed by the relation $z = \ln z$, the equation of the boundary surface is easily derived giving $z = -\frac{1}{2} \ln \left(1 + (e^{-2a} - 1) \sin^2 y\right)$
This approximates closely the outline of the granite surface in giving the bonches on each side.

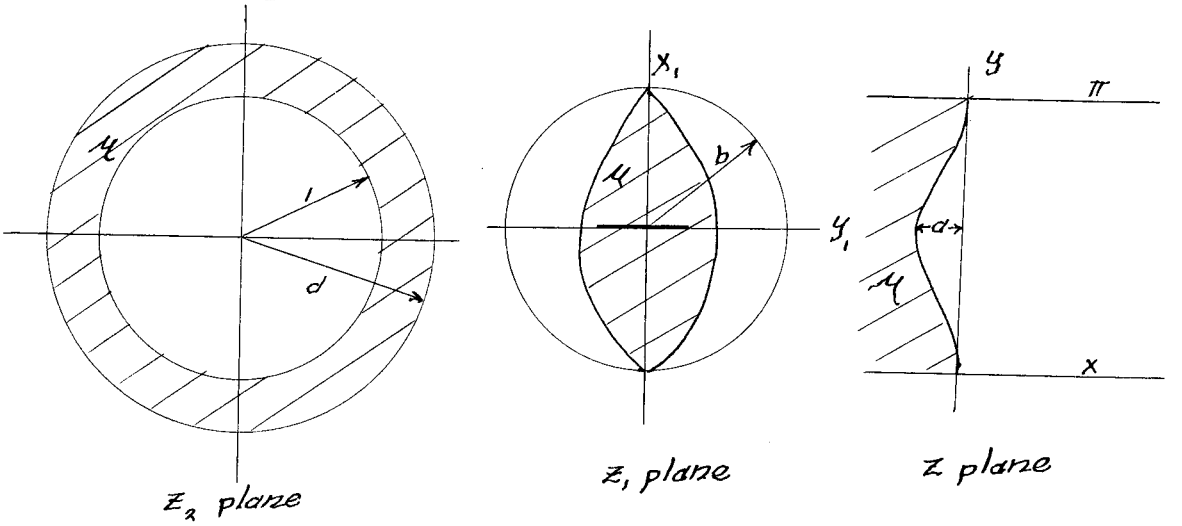

In this case the horizontal field gives radial lines which are tangential to the axis normally. By a second transformation $Z_1 = c\left(\frac{1 + Z_2}{Z_2}\right)^2$ enables one to

transform the elliptical boundary into a circular one and b/ proper evaluation of the boundary conditions and the use of circular harmonics one may get a solution that is cumbersome to evaluate accurately.

CASE II

This case is not as good an approximation, but gives the desired analysis. One may transform a circle into the z plane.

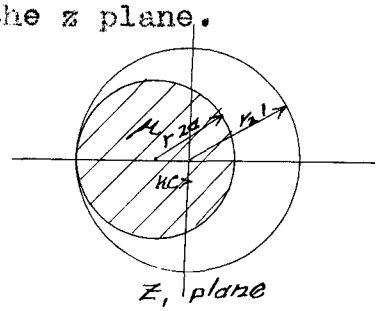

$z = \ln Z_1$

$Z_1 = e^z$

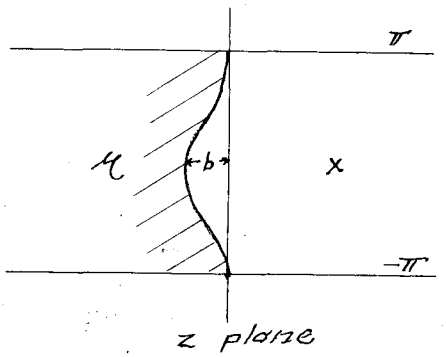

Now $x + iy = e^x(\cos y + i \sin y)$

$(x_1 + c)^2 + y_1^2 = a^2 = (1+c)^2$

$e^{2x} + 2c e^x \cos y = 1 - 2c$

when $Z_1 = a - c_1$ $z = -b$, so $c = \frac{1 - e^{-b}}{2}$

and equation of boundary is

$$x = \ln \left\{ \sqrt{e^{-b} + \frac{(1-e^{-b})\cos^2 y}{y}} - \frac{(1-e^{-b})}{2} \cos y \right.$$

$$y = \cos^{-1} \frac{e^{-b} - e^{2x}}{e^x(1-e^{-b})}$$

in the z plane the potential is given by

$$W = H\cos\alpha\, x - jH\sin\alpha\, y$$

$$= He^{-j\alpha z} = He^{-j\alpha}\ln z_1 = HE\ln z_1 \quad \text{where } E \text{ is complex}$$

This form of potential enables one to use the theory of images[6],

In the z_1 plane, then, we have the potentials given by a line charge at z = 0, an image at $\frac{a^2}{c}$ where c is the distance of the center of the cylinder from the origin and one at the center to keep the total charge the same. Potential outside of the cylinder then is:

$$W_1 = HE\ln z_1 + AH\ln(z_1 + c)$$

Potential inside of the cylinder:

$$W_2 = HB\ln z_1 + H + c\ln\left(z_1 + c - \frac{a^2}{c}\right) + D$$

putting $z_2 = z_1 + c$, we have

$$W_1 = H\left\{E\ln\left(1 - \frac{c}{z_2}\right) + (A+E)\ln z_2\right\}$$

$$W_2 = H\left\{B\ln\left(1 - \frac{c}{z_2}\right) + c\ln\left(1 - \frac{cz_2}{a^2}\right) B\ln z_2 - c\ln\frac{a^2}{c} + D\right\}$$

$$W_1 = H\left\{\sum_1^\infty \frac{(-1)^n E c^n}{n r_2^n}(\cos n\theta_2 - j\sin n\theta_2) + (A+E)\ln r_2 + (A+E)i\theta_2\right\}$$

$$W_2 = H\left\{\sum_1^\infty \frac{(-1)^n B c^n}{n r_2^n}(\cos n\theta_2 - j\sin n\theta_2) + \quad r_2^n(\cos n\theta_2 + j\sin n\theta_2)\right.$$

$$\left. + B\ln r_2 + Bi\theta_2 - c\ln\frac{a^2}{c} - c\pi i + D\right.$$

Taking real part

$$U_1 = H\left\{\sum_1^\infty \frac{(-1)^n c^n}{n r_2^n}(E_R\cos n\theta_2 + E_I\sin n\theta_2) + (E_R + A_R)\ln r_2 - (A_I + E_I)\theta_2\right\}$$

$$U_2 = H\left\{\sum_1^\infty \frac{(-1)^n}{n}\left[\frac{c}{r_2^n}(B_R\cos n\theta_2 + B_I\sin n\theta_2) + \frac{c^n r^n}{a^{2n}}(C_R\cos n\theta_2 - C_I\sin n\theta_2)\right.\right.$$

$$\left.\left. + B_R\ln r_2 + C_R\ln\frac{a^2}{c} - B_I\theta_2 - C\pi + D\right.\right.$$

where $\bar{E} = E_R + j E_I$ The subscript R refers to the real part, and the subscript I refers to the imaginary part of the complex variable.

The boundary conditions are:

$$r = a \qquad u_1 = u_2$$

$$\frac{\partial u_1}{\partial r} = \mu \frac{\partial u_2}{\partial r}$$

Which gives the equations:

1) $A_I + E_I = B_I$
2) $E_I + C_I = B_I$
3) $E_I = \mu (B_I + C_I)$
5) $E_R = B_R + C_R$
6) $E_R = \mu (B_R - C_R)$
7) $A_R + E_R = \mu B_R$
4) $(A_R + E_R) \ln a = B_R \ln a + C_R \ln \frac{a^2}{c} - C\pi + D$

Solving these we get for the coefficients

$$B = \frac{\mu + 1}{2\mu} (E_R + j E_I)$$

$$C = \frac{\mu - 1}{2\mu} (E_R + j E_I)$$

$$A = \frac{\mu - 1}{2} (E_R - j \frac{E_I}{\mu}$$

and

$$W_1 = H \left\{ (E_R + j E_R) \ln Z_1 + \frac{\mu - 1}{2} (E_R - \frac{j}{\mu}) \ln (Z_1 + c) \right.$$

as $z \to \infty$

$$W_1 = H \left\{ E_R \left(\frac{\mu + 1}{2}\right) \ln Z_1 + j E_I \left(\frac{\mu + 1}{2\mu}\right) \ln Z_1 \right.$$

$$= H e^{-j\alpha} \ln Z_1$$

so that

$$E_R = \frac{2\cos\alpha}{\mu+1}\ ,\quad E_I = -\frac{2\mu\sin\alpha}{\mu+1}$$

and W_1 reduces to

$$W_1 = H\left\{(E_R + jE_I)\,z + \left(\frac{\mu-1}{2}\right)\left(E_R - \frac{jE_I}{\mu}\right)\ln\left(e^z + \frac{(1-e^{-b})}{2}\right)\right.$$

the field is $\frac{dW_1}{dz} = H\left\{E_R + jE_I + \frac{\mu-1}{2}\left(E_R - \frac{jE_I}{\mu}\right)\left(\frac{e^z}{e^z + \frac{1-e^{-b}}{2}}\right)\right.$

Now the real part of this is the vertical field and the imaginary part is the horizontal field. Thus

$$H_x = \frac{H}{\mu+1}\left\{2\cos\alpha + \frac{(\mu-e^x)}{e^{2x} + (1-e^{-b})\cos y + (1-e^{-b})^2}\left(\cos\alpha\left(e^x + \left(1-\frac{e^{-b}}{2}\right)\cos y\right) - \sin\alpha\left(\frac{1-e^{-b}}{2}\right)\sin y\right.\right.$$

$$H_y = \frac{H}{\mu+1}\left\{2\mu\sin\alpha + \frac{(\mu-1)e^x}{e^{2x} + (1-e^{-b})\cos y + \left(\frac{1-e^{-b}}{2}\right)^2}\left(\cos\alpha\left(1-\frac{e^{-b}}{2}\right)\sin y + \sin\alpha\left(e^x + \left(\frac{1-e^{-y}}{2}\right)\cos y\right)\right.\right.$$

CALCULATIONS

The basin was assumed to be 40 miles long and 40,000 feet deep at the center. A field of 0.5 gauss, inclined at 30° to the vertical was used. A permeability of 1.012 for the granite is used. Thus

$\mu + 1 = 2.012$ $\qquad e^{-b} = 0.301$

$\mu - 1 = 0.012$ $\qquad H = 0.5$ gammas

$\cos\alpha = 0.866$

$\sin\alpha = 0.500$

and the equations for the x and y components of the field intensities are:

$$H_x = 0.5\left\{0.8650 + \frac{0.006\,e^x}{(e^{2x} + 0.70\cos y + 0.12}\left(0.866\,(e^x + 0.35\cos y) - 0.175\sin y\right)\right\}$$

$$H_y = 0.5\left\{0.505 + \frac{0.006\,e^x}{(e^{2x} + 0.70\cos y + 0.12}\left(0.50(e^x + 0.35\cos y) + 0.310\sin y\right)\right\}$$

In order to approximate actual field relations more closely, a traverse line of definite slope ($x = my + k$) was chosen.

Then one would have for the horizontal and vertical fields measured, contributions from the x and y components from the formula as:

where o is the angle that the line of traverse makes with x = 0. In the present case the angle 0 = tan is approximately 20°, so that the formula for the x and y components were used directly.

CONCLUSIONS.

The conclusions which may be drawn from this magnetic survey are as follows:

1. Attempts to locate the position of faults of considerable displacement covered by thicknesses of from 5,000 to 10,000 feet of aluvium, and other sedimentary formations, in the Los Angeles Basin were entirely unsuccessful.

2. Calculated values of the vertical and horizontal intensities of the magnetic field, after the method of Smythe and Uhrig, using as a theoretical cross-section one which has been compiled by R. A. Peterson from all available, gravity, seismic, and oil well log data, compare very well except in the vicinity of the San Pedro Hills. From the San Gabriel Mountains to the vicinity of the Inglewood Fault the greatest difference between the calculated and observed values of vertical intensity

is approximately 50 gammas and may be explained by the fact that in this part of the section the sinousoidal boundary used for the purpose of calculation is somewhat different from the hypothetical boundary between the granite and sedimentary formations. In this part of the section the calculated and observed values of the horizontal component of the field also agree very well. The difference of 100 gammas may be accounted for as was the difference between the calculated and observed values of the vertical component.

In the vicinity of the San Pedro Hills, or between the Inglewood fault and the Pacific Ocean, the calculated and observed values of both the horizontal and vertical components of the field, differ widely. The profile of the observed values of the vertical component drops from 200 gammas at the Inglewood Fault to a minimum of 40 gammas at the north side of the San Pedro Hills. The profile rises again to 150 gammas in the San Pedro Hills. The observed value of the vertical component of the field is approximately 300 gammas less than the calculated value. In this vicinity the observed value of the horizontal component of the field is nearly 600 gammas less than the calculated value. From these facts it may be concluded that the hypothetical geologic cross-section is incorrect for the San Pedro Hills vicinity. In order to satisfy the observed values of the magnetic field the hypothetical geologic cross-section should indicate a

much greater thickness of sediments or metamorphic rocks of low permeability than is shown on figure 1.

During the Long Beach earthquake, which occurred as a result of displacement along the Inglewood Fault, portable seismographs were stationed in the San Pedro Hills. Waves originating on the Inglewood Fault and recorded in the San Pedro Hills had velocities much lower than the velocity for granite, indicating that they travelled through rocks other than granite which is in accord with the above interpretation of the magnetic data.

The author wishes to acknowledge the helpful criticisms of Professors B. Gutenberg and J. P. Buwalda.

DATA SHEET

LOS ANGELES BASIN SURVEY

Vertical Component

Station	Reading	Temperature	Time
1*	19.6	20.3°C	10.19
2	22.1	20.5	11.05
3	20.8	21.8	11.25
4	18.3	23.0	11.51
1*	19.0	22.8	12.11
5	19.0	25.0	1.34
6	18.0	24.0	1.49
6A	19.1	23.0	1.57
7	18.6	22.0	2.14
8*	17.7	21.0	2.26
1*	19.7	21.5	2.48
8*	18.2	21.0	3.36
9	18.2	19.5	3.59
10	18.0	18.0	4.10
11	17.9	17.5	4.20
12	17.2	17.5	4.30
13	16.9	17.0	4.40
8*	19.6	16.3	4.51
1*	19.6	22.0	10.00
8*	17.3	23.0	10.20
14	14.6	23.0	10.38
15	13.0	23.0	10.49

Station	Reading	Temperature	Time
16	12.4	23.5°C	11.02
17	12.2	24.0	11.11
18	11.6	24.0	11.18
18	11.4	24.0	11.27
20	11.0	24.0	11.42
21	10.3	25.5	11.55
22*	9.8	25.0	12.05
8*	15.2	28.0	12.54
23	9.1	30.0	2.12
24	9.3	29.0	2.21
25	10.0	28.0	2.30
26	8.9	28.0	2.37
27	8.8	28.0	2.45
28	10.1	28.0	2.55
29	9.7	27.0	3.10
30	10.0	26.0	3.25
31	10.1	26.0	3.45
32	9.9	25.5	3.55
33	9.7	25.0	4.07
34	10.3	22.0	4.16
35*	10.5	21.0	4.34
22*	11.9	22.0	5.00
22*	12.0	19.5	10.23
36	13.7	19.0	10.44
37	12.1	19.0	10.52
38	11.4	19.0	11.00
39	10.9	20.0	11.15
40	11.2	20.0	11.21

Station	Reading	Temperature	Time
41	10.7	20.5°C	11.29
42	11.1	21.0	11.39
43	11.8	21.5	11.52
44	9.8	21.5	12.09
45	9.8	22.0	12.50
46	10.0	22.0	1.00
47	8.8	22.0	1.07
48	9.8	22.0	1.15
49	11.9	22.0	1.28
50	11.0	22.0	1.45
51	10.8	21.5	1.54
52	10.6	22.0	2.07
53	9.9	21.5	2.15
54	10.1	21.5	2.25
22*	11.8	20.5	2.51
22*	12.1	17.5	10.04
55	10.3	20.5	11.14
56	11.2	21.0	11.30
57	10.2	20.0	11.39
58	10.7	20.0	11.45
35*	9.0	21.0	12.42
59	9.3	21.0	12.59
60	9.0	21.0	1.15
61	8.7	21.0	1.26
62	8.5	21.0	1.37
63	8.9	21.0	1.52
64	8.8	21.0	2.06
65	8.6	20.5	2.20

Station	Reading	Temperature	Time
66	8.2	21.0°C	2.32
67	7.7	20.0	2.57
68*	8.0	19.0	2.11
35*	10.8	19.5	3.39
68*	7.1	20.5	10.19
69	6.3	20.5	10.35
70	7.6	22.5	10.45
71	6.1	24.0	11.03
72	5.9	24.5	11.15
73	5.4	25.0	11.36
74	3.9	25.0	11.54
75	2.5	25.0	12.07
76*	1.0	24.5	12.24
68*	7.2	26.5	1.10
76*	3.0	14.0	9.50
77	1.6	16.0	10.06
78	2.3	18.0	10.20
79	2.3	23.0	11.25
80	3.7	22.5	11.56
81	3.6	23.0	12.07
82	2.0	23.0	12.21
79A	3.8	24.0	12.36
76*	0.3	24.5	1.07
83	1.0	24.0	2.00
84	0.0	23.0	2.15
85	-1.4	23.0	2.36
86	-2.5	22.0	2.48
87	-1.1	22.0	3.04

Station	Reading	Temperature	Time
88	-1.7	21.0°C	3.19
89*	-2.4	21.0	3.32
76*	2.1	23.0	4.21
89*	-2.5	21.5	10.26
90	-2.2	21.0	10.35
91	-2.7	20.0	10.43
92	-3.1	20.0	10.51
93	-2.9	20.0	11.12
94	-3.9	20.0	11.24
95	-10.0	20.0	11.51
96	-4.3	20.0	12.06
97	-5.4	20.0	12.13
98	-3.5	20.0	12.25
89*	-2.9	20.0	12.42
99	1.1	22.0	1.51
100	3.7	20.0	2.15
101	3.7	20.0	2.27
102	7.0	20.0	2.40
103	5.5	20.0	2.55
6*	17.0	20.0	10.01
104	18.0	20.0	10.15
105	22.5	20.0	10.39
106	19.6	20.0	10.46
107	13.3	20.0	10.55
108	15.1	20.0	11.02
109	17.4	20.0	11.10
110	24.3	20.0	11.28
111	28.0	20.0	11.40

Station	Reading	Temperature	Time
112	15.7	20.0°C	11.50
113	12.3	20.0	11.59
114	9.9	21.0	12.15
115	22.7	25.0	2.02
8*	15.9	24.5	3.25
89*	19.2	18.0	9.15
116	0.2	20.0	1.30
117	-2.4	21.0	1.45
118	-3.0	20.0	2.05
119	-3.6	20.0	2.18
120	-2.5	18.0	3.00
121	-4.1	18.0	3.30

Horizontal Component

122*	2.4		9.35
123	5.6		10.00
124	-1.2		10.20
125	-3.3		10.30
122*	0.8		11.05
126	-3.8		11.45
128	-5.0		12.05
129	-0.5		12.35
130	1.4		12.50
122*	0.3		1.50
131	3.8		2.10
132	2.8		2.40

Station	Reading	Time
133*	2.2	2.55
134	-5.0	3.10
135	2.8	3.30
136	-0.9	3.45
137	-5.4	4.15
133*	0.9	4.25
122*	-0.9	4.40

Vertical Component scale factor 22 gammas

Horizontal Component scale factor 30 gammas

Temperature correction for vertical component add 4 gammas per degree over 20°C

FOOTNOTES

1. State of California, Water Supply Paper, Bull. #45. Southern California #15, Guidebook of 16th International Geological Congress.

2. B. Gutenberg, H. O. Wood, and J. P. Buwalda, Experiments Testing Seismographic Methods For Determining Crustal Structure. Bulletin Seismological Society of America, Vol. 22, 1932, B. Gutenberg and J. P. Buwalda, Seismic Profile Across Los Angeles Basin. Paper presented at meeting of Geological Society of America, Coord. Section 1935, Abstracts page 6.

3. R. A. Peterson, Results of Gravity Measurements in Southern California. Unpublished Doctor's Thesis, 1935, California Institute of Technology.

4. J. L. Soske, Unpublished Doctor's Thesis, California Institute of Technology.

5. Jeans, The Mathematical Theory of Electricity and Magnetism, pgs. 186 - 201.

PART II

MAGNETIC SURVEY OF ANTELOPE VALLEY, CALIFORNIA

MAGNETIC SURVEY OF ANTELOPE VALLEY

INTRODUCTION

Since attempts to trace faults with the magnetometer were unsuccessful in the Los Angeles Basin Area, because of the great thicknesses of sediments, Antelope Valley was selected for study in the hope that some of the numerous faults crossing this area would yield positive results. As work progressed the character of anomalies encountered suggested that a general survey of the entire valley region might lead to interesting results so the survey was extended and data gathered in the sufficient quantities for the purpose of constructing a map of lines of equal magnetic anomaly.

GEOGRAPHY

Antelope Valley lies approximately 60 miles due north of the city of Los Angeles. It is bounded on the south by the San Gabriel Mountains and on the northwest by the Tehachapi Mountains. To the northeast lies the great Mojave Desert.

The towns of Palmdale and Lancaster are located in the valley on the line of Southern Pacific railroad. Much of this desert valley has been made excellent farming land by means of irrigation.

GEOLOGY

The California Bureau of Mines Mineralogists Report XXX, includes a geologic map of Antelope Valley which was used by the writer as a guide in this study.

The geology of the area north of the San Gabriel Mountains is relatively simple. The valley is underlain by granitic rocks covered with varying thicknesses of alluvium and continental sediments. With the exception of two localities, at Antelope Buttes and Little Buttes, there are no rock exposures in the valley proper. At Antelope Buttes there is a large exposure of the granitic basement in contact with tertiary continental formations on the northwest side of the Buttes. In Little Buttes the same rocks are exposed.

Several extensive faults of considerable displacement are supposed to transect the area. The Rosamond Fault, which lies at the south base of the line of hills which separate Antelope Valley from the Mojave Desert, extends in an east-west direction. According to the work of Simpson the vertical displacement on this fault is approximately 2,000 feet. In the northwest corner of the valley there is mapped a branch of the Garlock Fault trending northeast-southwest along the southeast front of the Tehachapi Mountains. The vertical displacement on this fault is supposed to be approximately 2,500 feet.

North of the Rosamond Fault are exposed granite, tertiary flows and sediments.

MAGNETIC SURVEY

Rosamond Fault

This feature was selected as one which it should be possible to trace with a magnetometer. As may be seen by reference to the geologic map accompanying this report, the Rosamond Fault is mapped with a solid line in the vicinity of Willow Springs only, upon the surficial evidence of a scarp in the aluvium. From Willow Springs eastward the fault is mapped with a dashed line indicating its exact location is questionable.

Eight profiles were made across the supposed location of the fault spaced at intervals of from two to three miles. These profiles are all quite anomalous in character. The intensity of the vertical component is much greater in the southern portions of the profiles than in the northern parts. The maximum difference in intensity being approximately 300 gammas. A study of the profiles reveals that the steepest gradients of intensity occur near stations (see isomagnetic map in envelope of back cover) 78, 39, 105, 605 and 612. Due to the occurrence of lavas on the northern portions of these profile lines the anomalous character of the profiles is not due simply to the displacement of the granite,

however, at the stations mentioned above the steep gradients are considered to be due to the displacement of the granite. The dashed red line through these points then, marks the probable location of the trace of the Rosamond fault as interpreted from magnetic data. It is seen to coincide with the geologic interpretation in the vicinity of Willow Springs, but deviates southward to the east of this point. The fact that the trace of the fault, as indicated by the magnetic survey, continues in the same direction as the known part of the geologically determined fault trace is significant.

Garlock Fault

The geological map of Antelope Valley indicates, by a dashed line, the trace of a branch of the Garlock Fault, and the cross-section shows a displacement of approximately 2,500 feet. Surficial evidence for the existence of this fault is found in the eluvial scarp and drag fold seen two miles north of the Antelope Valley Pumping Station in T 9 N R 15 W. Attitudes in this structure indicate a post alluvium displacement of approximately 250 feet. It is reasonable to believe the total vertical displacement of this fault to be much greater.

Measurements of the vertical component of the field were made on the profile lines crossing the supposed

location of this fault trace. The profiles are without any anomaly which might be indicative of a fault. A fault of from 250 to 500 feet displacement at a depth of from 1000 to 2000 feet might not cause sufficient distortion of the field to yield a well defined anomaly in the measurement of the vertical component. However, a fault of 2000 feet displacement at a depth of 1000 feet or less, involving sediments and granite, should cause sufficient distortion to be decidedly noticeable in the measurements of the vertical component of the field.

The author suggests that this fault may not have as great a vertical displacement as has been previously supposed. Magnetic measurements indicate that the vertical displacement is probably not more than 500 feet.

General Magnetic Survey of Antelope Valley

Measurement of the vertical component of the field was made over the entire Antelope Valley area. The method of survey used was a system of north-south and east-west profile lines of measurements at intervals of from one to two miles except where appreciable differences in intensity were noticed in which case shorter intervals, one-quarter to one-half mile, were used to detail the anomaly. This method of reconnaisance proved to be a fast and efficient method of survey.

From data collected in this manner profiles

were drawn from which iso-magnetic lines, or lines of equal magnetic anomaly, were determined and sketched on the geologic map of the area. (See iso-magnetic map in pocket of rear cover.) The iso-magnetic interval used was 50 gammas of intensity.

The configuration of the iso-magnetic lines is considered to correspond to the configuration of the granitic basement rocks, or in other words, where the iso-magnetic lines indicate a high magnetic intensity the granite is near the surface and vice versa. Comparison with geologic data shows a magnetic "high" to exist in the region of Antelope Buttes and Little Buttes where there are low hills of granite. Trending in a general east-west direction just south of the Rosamond Fault is an elongated magnetic "high" which, on the basis of the comparison made above between the magnetic "high" and granitic outcrop, may be considered to indicate the configuration of a granite ridge lying not deeply buried below the surface.

The lowest levels of the buried granite surface, as indicated by the magnetic survey, lie just northwest of Antelope Buttes and east of Antelope and Little Buttes. In the area northwest of Antelope Buttes a bore-hole, in search of petroleum, reached granite at a depth of 3300 feet. In the area south-east of Antelope and Little Buttes several bore-holes have been dug to depths of more than 2000 feet without reaching the granite.

Six miles northwest of Willow Springs, in an area where the magnetic survey indicates that the granite lies at a great depth, the Regina Oil Corporation is now in the process of digging for oil. The hole is well over 3000 feet deep at present and granite has not yet been encountered.

As far as the writer is aware no bore-holes have been made in the area indicated as a magnetic "high."

CONCLUSIONS

In this area considerable knowledge of the geologic structure was gained through the use of the magnetometer. The trace of the Rosamond fault was extended from a locality in which it was established from surficial evidence to a locality where no surficial evidence exists. The branch of the Garlock fault, in the northwest part of the area, was determined to have a smaller vertical displacement than previously considered. The general magnetic survey yields information regarding the relative depths to the granitic basement in the area. It may be concluded that the magnetic method was extremely useful as an aid to the solution of geologic structure in Antelope Valley.

Sidney Schafer
California Institute
May, 1936

DATA SHEET

ANTELOPE VALLEY SURVEY

Vertical Component

Station	Reading	Temperature	Time
33*	-0.3	28°C	930
34	-4.9	28	940
35	-9.6	28.5	955
36	-10.3	29	1010
37	-11.6	29	1020
38	-13.2	30	1035
39	-13.5	31	1045
40	-13.7	32	1055
41	-13.5	32	1120
33*	-3.0	32	12:10
42	-5.9	32	1220
43	-3.9	32	1230
44	-1.2	32	1240
45	-1.4	32	1245
46	-0.8	33	12.55
47	-1.7	33	1.05
48	-6.6	33	1.15
49	-7.7	33	1.20
50	-7.3	34	1.30
51	-6.5	34	1.37
52	-6.8	34	1.50
33*	-3.1	34	2:00
33*	0.2	26	8:40
55*	-7.2	27	8.50

Station	Reading	Temperature	Time
56	-7.2	28°C	9:00
57	-13.3	29	9.05
58	-15.4	30	9.15
59	-17.1	30	9.20
60	-18.6	31	9.30
61	-19.9	31	9.40
62	-18.1	32	9.50
63	-16.2	32	9.55
64	-10.2	32	10:05
65	-11.0	33	10.15
66	- 7.0	33	10.20
67	- 8.1	33	10.40
68	- 8.2	33	10.40
69	-10.4	33	10.45
70	-11.4	34	10.55
71	-12.3	34	11.10
72	-12.5	34	11.25
55*	- 9.6	34.5	12:00
73	-12.7	33	1:05
74	-13.4	32	1:15
75	-14.0	32	1:30
33*	- 2.1	32	2.07
84	- 5.5	33	2.15
83	- 8.9	33	2.25
82	- 9.2	33	2.35
81	-7.5	33	2.45
80	-6.2	33	2.55
79	-7.4	33	3.05
78	-10.3	32	3.15

Station	Reading	Temperature	Time
77	-10.5	32°C	3.25
76	-10.8	32	3.35
85	- 2.8	32	3.50
86	- 3.2	32	4.05
87	- 2.6	31	4.15
88	- 1.2	31	4.25
89	0.5	31	4.30
90	0.2	31	4.35
91	- 3.2	30	4.45
92	- 4.5	30	5.00
93	- 4.7	29	5.10
94	- 4.9	29	5.20
33*	- 0.4	28.5	5.30
55*	4.2	22	9:45
95	7.6	24	10:00
96	7.3	26	10:09
97	0.1	26	10;16
98	0.3	26	10:27
99	9.8	26	10:36
100	10.1	26	10:46
100A	9.7	26	10.55
101	10.6	26	11:00
102	11.1	26	11:07
103	2.0	26	11:15
104	3.2	25	11:24
55*	3.5	26	12:00
55*	2.9	27	1:00
105	3.9	27	1:45

Station	Reading	Temperature	Time
106	5.3	27	1:55
107	3.2	26	2:00
108	0.2	26	2:08
109	0.1	26	2.16
110	1.8	26	2.24
111	4.9	26	2:30
112	10.5	25	2.40
113	10.1	25	2.48
114	10.0	25	3.00
105*	5.8	25	3.55
115	3.8	26	4:00
116	3.2	25	4:07
117	2.1	25	4.15
118	0.8	24	4.25
119	0.6	24	4.35
120	1.6	24	4.45
121	5.1	24	5.10
122	5.3	24	5.25
105*	6.0	20	6.00
3*	11.7	25	8:10
123*	0.0	26	8:56
124	0.0	27	9.00
125	0.2	27	9:10
126	0.3	28	9.15
127	0.6	28	9.21
128	0.6	29	9:30
129	0.9	30	9.40
130	1.5	30	9.50
131	1.5	30	9.55

Station	Reading	Temperature	Time
132	1.0	30°C	10.00
133	0.7	31	10.05
134	0.3	31	10.10
135	-0.7	31	10.15
136	-0.4	31	10.20
137	-0.8	32	10.30
138	-0.7	32	10.35
139	-3.1	32	10.45
140	-0.5	32	10.53
141	2.0	32	11:00
142	4.2	32	11.10
143	5.0	33	11.15
144	7.6	33	11.25
33*	8.4	33	11.32
145	- 2.5	33	12:15
146	-3.2	34	12.55
147	- 3.3	35	1:00
33*	7.7	34	1:20
156	2.8	34	1:30
155	1.4	34	1.40
154	0.5	34	1.50
153	1.8	34	2.05
152	1.7	34	2.15
151	1.0	33	2.20
150	0.2	32	2.35
149	-0.6	31	2.45
148	-1.3	31	3:00
33*	8.3	32	3.35

Station	Reading	Temperature	Time
33*	8.3	32°C	3.35
565*	7.5	31	3.55
501	1.0	19	9.45
502	1.9	18	9.50
503	2.7	19	9.55
504	2.8	19	10.05
505	2.6	19	10.20
506	2.6	18	10.30
507	2.0	18	10.40
508	1.6	18	10.50
509	2.5	20	11.05
510	1.4	20	11.15
511	2.8	20	11.25
512	2.8	26	
513	5.1	25	
514	5.2	25	
515	5.0	25	
516	4.6	26	
517	4.4	24	
518	3.9	24	
519	3.2	22	
520	3.0	21	
521	2.1	20	
522	1.6	20	
523	1.5	21	
524	0.6	21	
525	1.0	20	
526	3.5	20	
527	3.0	20	

Station	Reading	Temperature	Time
528	2.1	20°C	
529	1.7	20	
33*	12.5	22	
530	-1.1	18	9.00
531	-1.6	21	
532	-1.6	22	
533	-2.4	24	
534	-3.2	25	
535	-3.9	25	
536	-5.9	26	
537	-7.1	27	
538	-8.2	26	
539	-9.5	25	
540	-12.1	26	
541	-11.1	25	
542	-12.7	25	
543	-13.1	25	
544	-13.3	26	
545	-9.0	26	12.30
546	-13.0	27	
547*	5.3	27	
548	3.8	27	
549	-0.9	27	
550	-4.0	27	
551	-5.0	27	
552	-4.7	27	
553	-3.2	26	
554	-0.8	26	
555	-1.2	26	
556	-2.7	26	

Station	Reading	Temperature	Time
557	- 9.2	26°C	
558	- 6.6	26	
559	- 5.9	26	
547*	6.0	26	
560	1.9	26	
561	6.0	26	
562	7.2	26	
563	4.0	27	
564	2.6	27	
33*	10.2	27	3.30
33*	8.3	32	3.35
565	- 7.5	31	3.55
565*	- 0.8	30	12.00
566	- 1.7	32	12.15
567	- 1.0	32	12.25
568	- 1.7	33	12.32
569	1.4	33	12.45
570	11.0	33	12.55
571	6.5	33	1.00
547	15.7	33	1.07
572	9.9	34	1.12
573	6.4	34	1.20
574	4.5	35	1.30
575	4.3	35	1.35
576	5.2	35	1:45
577	3.0	36	1:50
578	3.0	36	2.05
579	6.3	36	2.15
580	3.1	37	2.20

Station	Reading	Temperature	Time
581	5.1	37°C	2.20
582*	4.9	37	2.45
565*	-2.2	37	3.00
583	0.0	37	3.15
584	0.7	37	3.20
585	1.0	37	3.30
586	1.9	37	3.40
587	1.2	37	3.50
588	0.8	37	3.55
589	-1.0	37	4.00
590	3.1	37	4.10
591	3.3	36	4.20
592	2.5	35	4.30
593	3.4	34	4.35
594	6.3	33	4.50
595	6.9	34	4.55
596	4.1	34	5.05
597	4.6	35	5.15
598	4.2	35	5.20
582*	6.6	35	5.30
582*	7.8	27	8.00
599	8.0	29	8.20
600	10.3	31	8.40
601	20.6	32	8.50
602	13.6	32	9.00
603	15.6	33	9.10
604	17.3	34	9.15
605	12.8	34	9.25
606	10.1	34	10.00

Station	Reading	Temperature	Time
607	6.8	34°C	10:05
608	7.0	34	10.10
609	7.0	34	10.25
610	8.0	34	10.35
611	7.6	35	10.45
612	6.3	35	10.50
613	12.0	35	11.00
614	11,1	34	11.05
615	9.6	34	11.10
616	5.8	34	11.20
617	9.9	34	11.25
618	11.0	34	11.30
619	8.1	34	11.35
620	4.3	34	11.45
621	6.7	34	11.55
582*	4.8	35	12.05
622	2.7	36	12.45
623	0,4	36	12.55
624	0.3	37	1.05
625	-3.0	37	1.15
626	-3.6	37	1.25
627	-3.9	36	1.30
628	-0.6	36	1.35
629	-2.8	35	1.45
630	0.5	35	2.00
631	0.7	35	2.10
632	0.8	35	2.20
633	0.4	35	2.25
634	0,0	35	2.30

Station	Reading	Temperature	Time
635	1.9	34°C	2.40
636	3.0	34	2.50
637	6.4	34	3.00
638	6.8	35	3.10
639	8.4	35	3.20
640	9.2	35	3.35
641	5.0	34	3.45
642	5.6	34	3.50
643	6.0	34	3.55
644	8.2	34	4.00
645	6.9	33	4.20
646	5.7	33	5.00
647	6.9	32	5.15
582	7.0	31	5.30
648	1.7	29	5.55
649	-1.7	29	6.05
650	-7.9	26	6.15
565*	0.6	24	10.40
651	0.4	26	10.55
652	4.0	25	11.10
653	10.7	25	11.20
542	10.0	25	11.30
595	7.1	27	11.55
654	15.0	28	12.05
655	9.1	28	12.20
656	14.7	29	12.30
33*	20.8	29	12.45
529	9.0	29	12.50
630	13.3	35	2.15

Station	Reading	Temperature	Time
631	13.7	33°C	2.20
632	13.5	33	2.30
633	16.7	31	2.40
634	19.0	30	2.55
635	23.6	27	3.05
636	26.5	27	3.15
637	33.5	27	3.30